Rate Coefficients of the Reactions of Chlorine Atoms with Haloethanes of Type CH3CCl3-xFx (x = 0, 1, and 2): Experimental and ab Initio Theoretical Studies

ARTICLE *in* THE JOURNAL OF PHYSICAL CHEMISTRY · APRIL 1996

Impact Factor: 2.78 · DOI: 10.1021/jp9603243

Rate Coefficients of the Reactions of Chlorine Atoms with Haloethanes of Type $CH_3CCl_{3-x}F_x$ (x = 0, 1, and 2): Experimental and ab Initio Theoretical Studies

A. Talhaoui, F. Louis, P. Devolder, B. Meriaux, and J.-P. Sawerysyn*

Laboratoire de Cinétique et Chimie de la Combustion, URA-CNRS 876, Université des Sciences et Technologies de Lille, 59655 Villeneuve d'Ascq France

M.-T. Rayez and J.-C. Rayez

Laboratoire de Physico-Chimie Théorique, URA-CNRS 503, Université de Bordeaux, 33405 Talence, France

Received: February 1, 1996; In Final Form: April 1, 1996[⊗]

The absolute rate coefficients for the hydrogen abstraction reactions from CH_3CCl_3 (k_1), CH_3CCl_2F (k_2), and CH_3CClF_2 (k_3) by chlorine atoms in gas phase have been measured as a function of temperature using the discharge flow/mass spectrometric technique (DF/MS). The reactions were investigated under pseudo-first-order conditions with Cl atoms in large excess with respect to the haloethanes. The temperature dependence of the rate coefficients is expressed in the Arrhenius form: $k_1(298-416\text{K}) = (2.8^{+4.1}_{-1.7}) \times 10^{-12} \exp[-(1790 \pm 320)/T]$, $k_2(299-429\text{K}) = (3.0^{+2.4}_{-1.3}) \times 10^{-12} \exp[-(2220 \pm 150)/T]$, $k_3(298-438\text{K}) = (1.5^{+3.1}_{-1.0}) \times 10^{-12} \exp[-(2420 \pm 400)/T]$. The units of the rate constants are cm^3 $molecule^{-1}$ s^{-1}, and the quoted uncertainties are $\pm 2\sigma$. For understanding the reaction path mechanism of the chlorination of the studied halogen-substituted ethanes, ab initio molecular orbital calculations were performed. Transition state structures were determined. These calculations lead to predictions of preexponential factors in the same order of magnitude of measured values. The ab initio energetics of the reactions were corrected using the ISO-M method, a mixing of isodesmic reactions for obtaining reaction enthalpies and concept of intrinsic energy of Marcus to deduce activation energies. A reasonably good agreement with the experimental values were found.

Introduction

In order to assess the environmental acceptability of the hydrochlorofluorocarbons (HCFCs) and hydrofluorocarbons (HFCs) proposed to replace the fully halogenated chlorofluorocarbons (CFCs) in industrial applications, many experimental investigations in recent years have been devoted to the determination of the rates and mechanism of the reactions of HCFCs and HFCs with the tropospheric constituents. Although these investigations have been mainly focused on the attack of HCFCs and HFCs by OH radicals and on the fate of the derived primary halogenated alkyl radicals under tropospheric conditions, some of the kinetic studies have been reported on the reactions of HCFCs and HFCs with chlorine atoms for two main reasons: (i) their use as sources of haloalkyl radicals and other subsequent radical species for laboratory studies involving the HCFCs and HFCs of interest; (ii) the assessment of the contribution of the removal processes of HCFCs and HFCs by Cl attack to the mean tropospheric lifetimes of these species.

If a number of recent rate coefficient measurements on the reactions of Cl atoms with HCFCs and HFCs have been performed at room temperature using various methods,[1−4] limited experimental data are available on the temperature dependence of these reactions. In a previous work, we have reported an experimental study[5] on the temperature dependence of the reactions of Cl atoms with halomethanes of type $CHCl_{3-x}F_x$. In this paper, we report the measurements of absolute rate coefficients as a function of temperature for the reactions of CH_3CCl_3 (140), CH_3CCl_2F (HCFC-141b), and CH_3CClF_2 (HCFC-142b) with chlorine atoms:

$$Cl + CH_3CCl_3 \xrightarrow{1} HCl + CH_2CCl_3$$

$$Cl + CH_3CCl_2F \xrightarrow{2} HCl + CH_2CCl_2F$$

$$Cl + CH_3CClF_2 \xrightarrow{3} HCl + CH_2CClF_2$$

Furthermore, as previously achieved for the hydrogen abstraction from nine halogen-substituted methanes (F, Cl) by chlorine atom attack,[6] we have carried out ab initio calculations in order to gain insight into the reactivity trends in the series of haloethanes of type $CH_3CCl_{3-x}F_x$. Transition state structures are determined and calculated kinetic parameters (activation energies and Arrhenius *A*-factors) are compared with the experimental values determined in this work. Reactivity trends along the series of studied compounds are also inspected and discussed.

Experimental Section

Method. The experiments were performed by using the conventional discharge flow/mass spectrometric technique (DF/MS). The apparatus has been already described in detail elsewhere.[5,7]

Chlorine atoms were generated by a microwave discharge in a mixture of Cl_2/He through a fixed side arm located in the upstream part of the flow tube. In order to minimize the loss of Cl atoms on Pyrex surfaces, all internal surfaces of the flow tube were coated with pure orthophosphoric acid. Initial concentrations of chlorine atoms were determinated by mass spectrometric measurement on the extent of Cl_2 to Cl conversion and occasionally by titration with C_2H_3Br as proposed by Park et al.,[8] both methods leading to results in good agreement.

[⊗] Abstract published in *Advance ACS Abstracts,* July 1, 1996.

S0022-3654(96)00324-3 CCC: $12.00

Flow rates of different gases were regulated by calibrated mass flow controllers. Average flow velocities were over the range of 2−9 m s^{-1}. The pressure in the flow tube (range, 2−5 Torr) was measured upstream and downstream by a capacitance manometer.

Monitoring of the Reactions. All experiments were carried out under pseudo-first-order conditions with chlorine atoms in large excess with respect to the initial concentration of the studied haloethane. Kinetic measurements were performed by monitoring the temporal decay of the intensity of the base peak ($CH_3CCl_{2-x}F_x^+$) corresponding to each haloethane. CH_3CCl_3 was detected at the mass/charge ratio $m/e = 97$ corresponding to the fragment ion $CH_3C^{35}Cl_2^+$, CH_3CCl_2F at $m/e = 81$ ($CH_3C^{35}ClF^+$) and CH_3CClF_2 at $m/e = 65$ ($CH_3CF_2^+$). These fragment ions (detected at 40 eV) are specific to the respective haloethane.

Compared to the alternative pseudo-first-order conditions where the haloethane is in large excess with respect to chlorine atoms, the present approach offers a more advantageous operation of the mass spectrometer/kinetic apparatus, both in specificity and sensitivity. Use of chlorine atoms as minor reactant requires measuring the temporal decay of the signal of $^{35}Cl^+$, the intensity of which can be contaminated by contributions from the fragmentation of all chlorinated species present in the reaction medium. To avoid additional contributions to the peak $m/e = 35$ assigned to the chlorine atom, it is necessary to operate at low electron energy (<20 eV), leading to a significant lowering of the sensitivity of the mass spectrometer.

Purities. The purities of HCFCs supplied by Solvay were >99.96% for HCFC-141b and >99.99% for HCFC-142b. CH_3CCl_3 (>99.0%) was obtained from Aldrich. These haloethanes were used without further purification. The source of Cl_2 was a commercial mixture (Alphagaz) constituted of 2% of Cl_2 (>99.99%) in helium (>99.9995%). As an additional diluent, helium (Air Liquide, purity > 99.995%) was purified by circulating through a liquid nitrogen trap.

Treatment of Kinetic Data. For the bimolecular reaction

$$Cl + CH_3CCl_{3-x}F_x \rightarrow HCl + CH_2CCl_{3-x}F_x$$

the consumption rate equation of the haloethane is defined as

$$-\frac{d[CH_3CCl_{3-x}F_x]}{dt} = k[CH_3CCl_{3-x}F_x][Cl] \qquad (1)$$

with k the bimolecular rate constant.

Under the pseudo-first-order conditions where $[CH_3CCl_{3-x}F_x]_o \ll [Cl]_o$, the consumption of chlorine atoms due to the reaction with the haloethane can be neglected and, in a first step, the temporal Cl concentration can be assumed constant and equal to $[Cl]_0$ along the flow tube. $[CH_3CCl_{3-x}F_x]_o$ and $[Cl]_o$ are respectively the initial concentrations of $CH_3CCl_{3-x}F_x$ and Cl. The rate equation (1) is usually simplified as follows:

$$-\frac{d[CH_3CCl_{3-x}F_x]}{dt} = k[CH_3Cl_{3-x}F_x][Cl]_o \approx k_{obs}[CH_3Cl_{3-x}F_x] \qquad (2)$$

with $k_{obs} = k[Cl]_0$, the pseudo-first-order rate constant.

The integration of eq 2 gives

$$\ln[CH_3CCl_{3-x}F_x] = -k_{obs}t + \text{constant} \qquad (3)$$

If plots of $\ln[I(CH_3CCl_{2-x}F_x^+)]$ versus reaction time for different initial concentrations of chlorine atoms, at constant temperature, are well-fitted to straight lines, the concentration of chlorine atoms can be considered fairly constant along the reaction distance. The conventional treatment of kinetic data obtained under pseudo-first-order conditions can be then applied. The slopes obtained using the least squares treatment from the plots $\ln[I(CH_3CCl_{2-x}F_x^+)]$ versus reaction time yield values of the pseudo-first-order rate constant k_{obs} for the respective $[Cl]_o$ concentrations. These results are then evaluated by plotting k_{obs} versus $[Cl]_o$ and fitting the results to a line the slope of which is taken as k.

Inspection of the plots $\ln[I(CH_3CCl_{2-x}F_x^+)]$ versus reaction time can reveal some deviations of experimental values, with respect to the mean straight line, for long reaction times and/or for high initial concentrations of chlorine. This behavior suggests the occurrence of secondary reactions, modifying the concentration of chlorine atoms along the reaction distance. As the consumption of chlorine atoms due to the primary reaction can be neglected under pseudo-first-order conditions, the variation of Cl concentration is generally attributed to homogeneous and heterogeneous recombinations of chlorine atoms in large excess:

$$Cl + Cl + He \xrightarrow{k_r} Cl_2 + He \qquad (a)$$

$$Cl \xrightarrow{k_w} {}^1/_2Cl_2 \qquad (b)$$

where k_r is the three body gas phase recombination rate constant and k_w the wall decay rate constant. As shown in an earlier work,[5] the temporal variation of the Cl concentration along the reaction zone due to their homogeneous and heterogeneous recombinations is to be taken into account for the treatment of kinetic data. Instead of using the eq 3 for determining k_{obs}, then the bimolecular rate constant k from the plot k_{obs} vs $[Cl]_o$, it is needed to use the following relationship:

$$\ln[CH_3CCl_{3-x}F_x] = P \ln Q(t) + R \qquad (4)$$

with

$$P = k/2k_r[He]$$

$$Q(t) = 2k_r[He][Cl]_{o,o}(1 - \exp(k_w t)) + k_w$$

$$R = \text{integration constant}$$

Plots of $\ln[CH_3CCl_{3-x}F_x]$ vs $[\ln Q(t)]/2k_r[He]]$ are straight lines, and the slopes yield corrected values of the bimolecular rate constant k, then denoted as k_c. The rate constants k_r and k_w governing these processes have been determinated under our experimental conditions in a preliminary study.[9] The absolute concentration of chlorine atoms observed downstream at the outlet of the flow tube, defined by $[Cl]_{o,o}$, is evaluted by measuring the intensity of the signal assigned to $^{35}Cl_2^+$ ($m/e = 70$) with and without microwave discharge:

$$[Cl]_{o,o} = 2[[Cl_2]_{o,i} - [Cl_2]_{o,o}] \qquad (5)$$

$[Cl_2]_{o,i}$ represents the initial concentration of Cl_2 (discharge switched off) and $[Cl_2]_{o,o}$ the concentration of Cl_2 measured at the outlet of the flow tube with the discharge switched on.

Results and Discussion

$Cl + CH_3CCl_3 \rightarrow HCl + CH_2CCl_3$ (k_1). Typical plots of $\ln[I\ (CH_3CCl_2^+)]$ as a function of time at 298 K for different concentrations of chlorine atoms are shown in Figure 1. The values of $(Cl)_o$, reported in the caption of this figure correspond to the concentration of chlorine atoms measured at the outlet of the flow tube using the mass spectrometric measurement of

TABLE 1: Summary of the Relevant Experimental Conditions and Values of the Rate Coefficients k_1 (Uncorrected) and $k_{1,c}$ (Corrected by Incorporating the Wall Loss and Homogeneous Recombination Reactions of Cl Atoms) as a Function of Temperature for the Reaction Cl + CH_3CCl_3

T (K)	P (Torr)	expt	$[CH_3CCl_3]_o$[a] $\times 10^{-13}$	$[Cl]_{o,o}$[a] $\times 10^{-14}$	$(k_1 \pm 2\sigma)$[b] $\times 10^{15}$	$(k_{1,c} \pm 2\sigma)$[b] $\times 10^{15}$
298	2.5−5.1	11	0.92−3.07	3.45−21.57	9.2 ± 1.0	7.1 ± 1.1
331	2.8−4.7	6	0.76−2.66	5.03−16.92	15.8 ± 1.0	12.3 ± 1.0
361	2.6−4.8	6	0.72−2.31	3.90−16.62	24.0 ± 1.0	19.7 ± 1.0
390	2.6−5.0	6	1.91−3.59	3.69−16.29	31.1 ± 2.6	26.1 ± 3.1
418	2.5−4.9	5	1.97−3.81	3.60−14.57	44.5 ± 3.6	41.4 ± 4.4

[a] Concentrations are expressed in molecule cm^{-3}. [b] Units are cm^3 molecule^{-1} s^{-1}.

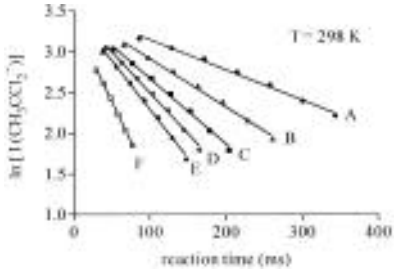

Figure 1. Typical plots of ln[$I(CH_3CCl_2^+)$] vs reaction time at 298 K. $[Cl]_o$ (10^{14} atoms cm^{-3}): A, 3.45; B, 7.02; C, 9.46; D, 11.65; E, 13.04; F, 21.57.

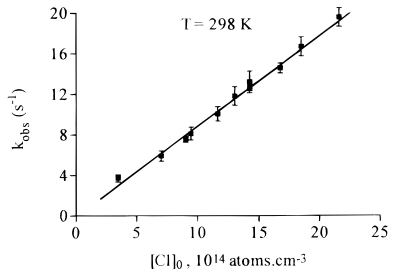

Figure 2. Pseudo-first-order rate constants k_{obs} plotted vs $[Cl]_o$ for the reaction Cl + CH_3CCl_3 at 298 K.

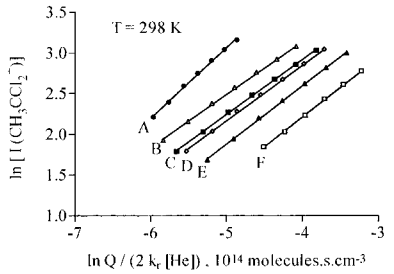

Figure 3. Plots of ln[$I(CH_3CCl_2^+)$] vs (ln Q)/2k_r[He], eq 4, to obtain $k_{1,c}$ incorporating heterogeneous loss, k_w, and homogeneous recombination, k_r, of Cl atoms. For the correction, the mean values of k_r and k_w (4.3×10^{-33} cm^{-6} molecule^{-2} s^{-1} and 0.7 s^{-1}, respectively) were used.

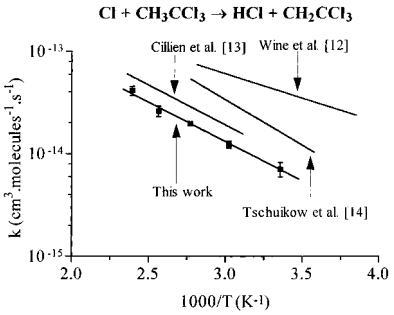

Figure 4. Comparison of different Arrhenius plots determined for the reactions of Cl atoms with CH_3CCl_3. The rate coefficients determined in this work at various temperatures were obtained as described in the caption of Figure 3.

Cl_2 to Cl conversion. In the framework of the usual treatment used for pseudo-first-order conditions, Cl concentrations are assumed constant along the reaction zone; i.e., recombination reactions of Cl atoms are considered negligible. It is worth pointing out that the correlation coefficients (r^2)for these straight lines range between 0.9964 and 0.9998, suggesting that the conventional pseudo-first-order treatment acceptable here. Least squares analysis yields values of the pseudo-first-order rate constant, k_{obs}, and the plot of k_{obs} vs $[Cl]_o$ gives the bimolecular rate constant k_1. Corrections due to radial and axial diffusion of CH_3CCl_3 have been applied to the values of k_{obs} reported in Figure 2. The following value is obtained for k_1:

$$k_1(298\text{K}) = (9.2 \pm 1.0) \times 10^{-15}\ \text{cm}^3\ \text{molecule}^{-1}\ \text{s}^{-1}$$

within statistical uncertainties of $\pm 2\sigma$ for the fit. A careful inspection of Figure 1 shows some deviations from linearity for experimental points corresponding to long residence times, suggesting homogeneous and heterogeneous recombination reactions of Cl atoms might be responsible for a significant decay of these atoms along the reaction zone.

In order to evaluate the impact of possible secondary reactions on the concentration profile of Cl atoms along the reactor, we have computed using a modeling program the [Cl] profiles due to the inclusion of reaction 1 and reactions a and b. This modeling shows that only homogeneous and heterogeneous recombination reactions a and b have a significant impact on the temporal evolution of Cl. Consumption of 10−37% of Cl atoms at 298 K is predicted at the end of the flow tube depending on the experimental conditions. This variation of Cl introduces a systematic error when the treatment of kinetic data without Cl loss is used. Accounting for the variation of Cl concentration, the plots obtained using the mean values of k_r and k_w are displayed in Figure 3 and the corrected rate coefficient $k_{1,c}$ is

$$k_{1,c}(298\text{K}) = (7.1 \pm 1.1) \times 10^{-15}\ \text{cm}^3\ \text{molecule}^{-1}\ \text{s}^{-1}$$

As expected, inclusions of Cl recombination reactions leads to a corrected value, $k_{1,c}$, lower than the uncorrected value, k_1. Compared to the values previously obtained at room temperature, our value is largely lower to the upper limit reported in the latest reviews,[10,11] which are only based on the value determined by Wine et al.[12] using a laser-flash photolysis/resonance technique. In this work, the value of k_1 is higher than expected because a significant fraction of the Cl atoms was removed by impurities. The results obtained here as a function of temperature are listed in Table 1. Rate constants for each temperature, results from the temporal variation of $[Cl]_{o,t}$,and mean values of k_r and k_w determined in this work have been used for the corrections. Least squares treatment of ln$k_{1,c}$ vs $1/T$ yields the following Arrhenius expression:

$$k_{1,c}(298\text{−}416\text{K}) = (2.8^{+4.1}_{-1.7}) \times 10^{-12} \exp[-(1790 \pm 320)/T]$$

The uncertainties correspond to 2σ. Figure 4 illustrates the Arrhenius plot obtained in this work compared with the

TABLE 2: Summary of the Relevant Experimental Conditions and Values of the Rate Coefficients k_2 (Uncorrected) and $k_{2,c}$ (Corrected by Incorporating the Wall Loss and Homogeneous Recombination Reactions of Cl Atoms) as a Function of Temperature for the Reaction Cl + CH_3CCl_2F

T (K)	P (Torr)	expt	$[CH_3CCl_2F]_o$[a] $\times 10^{-13}$	$[Cl]_{o,o}$[a] $\times 10^{-15}$	$(k_2 \pm 2\sigma)$[b] $\times 10^{15}$	$(k_{2,c} \pm 2\sigma)$[b] $\times 10^{15}$
299	3.1−4.5	6	1.36−2.22	1.05−1.95	2.1 ± 0.2	1.7 ± 0.2
328	3.9−4.8	6	1.02−2.52	1.13−2.15	4.5 ± 0.5	3.8 ± 0.3
353	2.2−4.9	6	1.34−2.29	0.97−1.93	6.1 ± 0.9	5.3 ± 0.9
373	3.4−5.3	7	1.27−2.43	0.95−2.13	8.7 ± 1.0	7.4 ± 0.8
402	3.5−4.8	7	1.07−2.34	0.86−2.05	13.4 ± 0.6	1.8 ± 0.5
429	3.6−5.6	7	1.26−2.12	0.90−2.23	20.1 ± 2.0	16.8 ± 2.0

[a] Concentrations are expressed in molecule cm^{-3}. [b] Units are cm^3 $molecule^{-1}$ s^{-1}.

TABLE 3: Summary of the Relevant Experimental Conditions and Values of the Rate Coefficients k_3 (Uncorrected) and $k_{3,c}$ (Corrected by Incorporating the Wall Loss and Homogeneous Recombination Reactions of Cl Atoms) as a Function of Temperature for the Reaction Cl + CH_3CClF_2

T (K)	P (Torr)	expt	$[CH_3CClF_2]_o$[a] $\times 10^{-13}$	$[Cl]_{o,o}$[a] $\times 10^{-15}$	$(k_3 \pm 2\sigma)$[b] $\times 10^{16}$	$(k_{3,c} \pm 2\sigma)$[b] $\times 10^{16}$
296	3.1−5.0	7	0.40−3.61	0.82−2.32	5.6 ± 1.1	4.7 ± 1.3
323	3.5−4.0	5	0.99−2.42	0.86−1.95	8.8 ± 2.0	7.8 ± 1.5
355	1.8−3.9	7	0.68−2.13	0.58−1.58	15.8 ± 3.6	14.2 ± 3.0
374	2.1−4.0	6	0.79−2.15	0.51−1.54	23.5 ± 6.6	22.6 ± 5.0
399	2.7−4.0	5	1.02−1.69	0.52−1.56	33.0 ± 10.0	32.6 ± 8.0
438	2.4−4.2	6	0.76−1.99	0.44−1.59	73.2 ± 10.0	68.2 ± 13.4

[a] Concentrations are expressed in molecule cm^{-3}. [b] Units are cm^3 $molecule^{-1}$ s^{-1}.

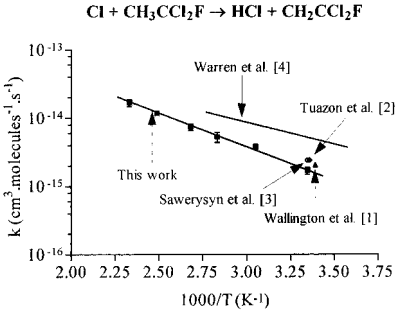

Figure 5. Comparison of different Arrhenius plots and values of the rate constant determined at room temperature for the reactions of Cl atoms with CH_3CCl_2F. The rate coefficients determined in this work at various temperatures were obtained as described in the caption of Figure 3.

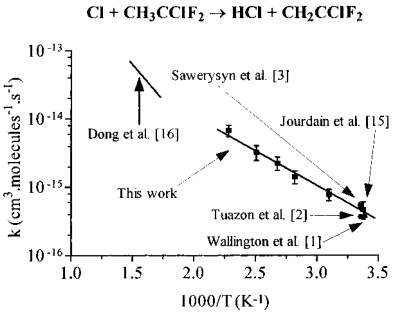

Figure 6. Comparison of different Arrhenius plots and values of the rate constant determined at room temperature for the reactions of Cl atoms with CH_3CClF_2. The rate coefficients determined in this work at various temperatures were obtained as described in the caption of Figure 3.

Arrhenius plots previously published in the literature. As shown in Figure 4, a good agreement is observed between our determination and the determination of Cillien et al.[13] using a relative method.

Cl + CH_3CCl_2F → HCl + CH_2CCl_2F (k_2). In a previous study,[3] we have determined for k_2 a value equal to $(2.1 \pm 0.2) \times 10^{-15}$ cm^3 $molecule^{-1}$ s^{-1} at 299 K without corrections for $[Cl]_o$ in a very good agreement (Figure 5) with the one obtained by Wallington et al.[1] and Tuazon et al.[2] using a relative rate method. As above, we estimate the systematic error due to the homogeneous and heterogeneous recombinations of Cl under our experimental conditions. Consumption of Cl at the end of the flow tube between 19.5 and 26.8% can be predicted at 299 K by modeling at the end of the flow tube. The kinetic data accounting for the Cl recombination reactions leads to a corrected value $k_{2,c}$ for k_2 very close to the uncorrected value:

$$k_{2,c}(298\text{K}) = (1.8 \pm 0.2) \times 10^{-15}\ \text{cm}^{-3}\ \text{molecule}^{-1}\ \text{s}^{-1}$$

Table 2 gives the results obtained for this reaction at various temperatures and relevant experimental conditions. By a least squares treatment of the plot $\ln k_{2,c}$ vs $1/T$, we obtain the following Arrhenius expression:

$$k_{2,c}(299-429\text{K}) = (3.0^{+2.4}_{-1.3}) \times 10^{-12} \times \exp[-(2220 \pm 150)/T]\ \text{cm}^{-3}\ \text{molecule}^{-1}\ \text{s}^{-1}$$

This Arrhenius expression is plotted in Figure 5. Our result is in relatively good agreement with the only earlier determination.

Cl + CH_3CClF_2 → HCl + CH_2CClF_2 (k_3). As previously published by the same group,[3] the treatment of kinetic data without correction for [Cl] loss leads to the value of $(5.7 \pm 0.4) \times 10^{-16}$ cm^3 $molecule^{-1}$ $s^{-1}$for the bimolecular rate constant k_3 at 298 K. Modeling calculations on temporal profiles of Cl show depletion can range between 7.5 and 21% depending upon experimental conditions. By incorporating the corrected $[Cl]_o$ in the corresponding plots $\ln[I(CH_3CF_2^+)]$ vs $\ln Q/2k_r[He]$, we obtain the following value for $k_{3,c}$:

$$k_{3,c}(296\text{K}) = (4.7 \pm 1.3) \times 10^{-16}\ \text{cm}^3\ \text{molecule}^{-1}\ \text{s}^{-1}$$

Comparisons to the previous measurements (Figure 6) show that this value is in good agreement with the value determined by Wallington et al.[1] and Tuazon et al.[2] by a relative rate method but remains within their uncertainty ranges. Our corrected value also exhibits good agreement with the previous value measured by Jourdain et al.[15] using the same experimental method but with no explicit account for variation of Cl concentration along the reaction distance.

Kinetic results at various temperatures and relevant experimental conditions are listed in Table 3. Linear least squares regression on data in the $\ln k_{3,c}$ vs $1/T$ plot (Figure 6) yields the Arrhenius expression

$$k_{3,c}(298-438\text{K}) = (1.5^{+3.1}_{-1.0}) \times 10^{-12} \times \exp[-(2420 \pm 400)/T]\ \text{cm}^3\ \text{molecule}^{-1}\ \text{s}^{-1}$$

To the best of our knowledge, this is the first Arrhenius expression reported for this reaction at lower temperatures to 500 K. The only one earlier Arrhenius expression has been determined by Dong et al.[16] in the temperature range 573−673 K using a relative method at 1000 Torr. As shown in Figure 6, their expression cannot predict the value of the rate constant determined at room temperature by different groups using various methods. Thermal decomposition of the halogenated ethanes used in this study could occur in the investigated temperature range.

Theoretical Study

The aims of these calculations are 2-fold: (i) showing that reliable rate parameter results can be predicted using medium size basis sets and standard levels of calculation and (ii) deducing the gross reactivity trends along the series of homologous compounds.

Used Methods. Ab initio calculations have been performed on hydrogen abstraction by chlorine attack from the compounds experimentally discussed here: namely, the series CH_3CCl_3, CH_3CCl_2F, CH_3CClF_2, and CH_3CF_3. Although the reaction $CH_3CF_3 + Cl$ has not been experimentally investigated in this work, we have decided to add it to the theoretical study in order to fulfill the series. The interest of this series lies in the analysis of the relative influence of the substitution from chlorine to fluorine on the secondary carbon to the abstraction of H atom in CH_3CX_3 (X = F, Cl) ethanes by a chlorine atom attack. This study will be compared to a similar previous one[6] on CHX_3 (X = F, Cl) where the substitution takes place directly on the carbon atom involved in the abstraction.

All of the calculations were performed using the Gaussian 92[17] software packages. All equilibrium and transition state structures were fully optimized at the Hartree−Fock level (RHF for closed shells or UHF for open shells) using the 6-31G(d) basis set.[18] The electron correlation energies were estimated by Møller−Plesset perturbation theory at the second order (MP2). The spin contamination has been taken into account by a projection method included in the Gaussian 92 program and will be noted in the results as PMP2. In our study, we consider that the transition state (TS) corresponds to the saddle point along the reaction path, a stationnary point characterized by only one negative eigenvalue of the Hessian matrix associated with an imaginary frequency in the normal mode analysis. A recent VTST study of the reaction $CH_4 + OH$[19] shows that the location of the saddle point along the minimum energy path is very close to the variational canonical transition state corresponding to the maximum free energy activation calculation. Using the optimized geometries of the stationary points, single point energies were calculated at the PMP2 level with the more extended basis sets 6-31G(d,p), 6-311G(2d,p), and 6-311G(2d,2p), the last one including 2p polarization functions located on each hydrogen atom. Finally, the PMP2/6-311G(2d,2p)//HF/6-31G(d) energies are corrected in an empirical way by a method fully described in an earlier paper[6] which was shown to lead to substantial improvements on the energetic values. This method is based (i) on the use of an isodesmic reaction to get a reliable determination of the enthalpy of the reaction of interest and (ii) on the concept of the intrinsic barrier of Marcus[20] to get an estimate of the activation enthalpy. Then, this method is now called the "ISO-M" method. For comparison, the energies have also been calculated using the BAC-MP4 program of Melius,[21] which takes as a starting point the MP4/6-31G(d,p)//HF/6-31G(d) values of the energies.

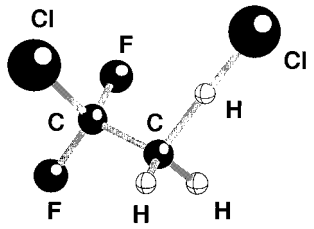

Figure 7. Drawing of one of the transition states ($F_2ClCC(H_2)-H-Cl$).

Results and Discussion. *(i) Structural Properties*. A saddle point has been found along the reaction path of the attack of the chlorine atom on the C−H bond of each substituted ethane. This saddle point is assumed to be the transition state (TS) of the reaction. As shown in Figure 7, the TS structures exhibit a nearly collinear arrangement of the three atoms involved in the exchange reaction, i.e., C, H, and Cl. The imaginary value of the frequency corresponds to an antisymmetric stretching of the C−H−Cl group. Optimized geometrical structures of the substituted ethanes and of the corresponding TS are gathered in Table 4. For the halogenated ethanes containing both fluorine and chlorine atoms, the H atoms of the CH_3 moities of CH_3CCl_2F and CH_3CClF_2 are not equivalent and then lead to two different TS. In the case of the $CH_3CCl_2F + Cl$ reaction, the lowest transition state corresponds to the abstraction of the H atom which is in a staggered position between the two chlorine atoms, whereas, in the case of the $CH_3CClF_2 + Cl$ reaction, it corresponds to the hydrogen atom in a staggered position between a fluorine and a chlorine atom. In the same way as in ref 6, listed in this table are the L parameters, defined as the ratio $L = \delta r(C-H)/\delta r(H-Cl)$, where δr(C−H) and δr(H−Cl) are the corresponding bond distance variations between the TS structure and the reactant CH_3CX_3 for the C−H bond and between the TS structure and the product HCl for the H−Cl bond. Recall that a value of L greater than 1 corresponds to a TS which presents a geometrical structure closer to the one of the product than to the reactant. By comparison with the results on L obtained in our previous study on the abstraction reactions on halogenated methanes,[6] it can be seen that L is, in this study, larger (from 1.58 to 1.68 compared with the values 1.06 to 1.35 found in this previous study, except for the reaction $CHF_3 + Cl$ where the value L =1.65 had been obtained—see Table 2 in ref 6). These transition states are then globally more productlike than the analogous structures involving halogenated methanes. As shown below, this result is consistent with the fact that the relevant reactions are less exothermic than the reactions with halogenated methanes, except for $CHF_3 + Cl$ and $CH_3CF_3 + Cl$ which have almost the same reaction enthalpy (respectively 3.7 and 4.0 kcal mol^{-1}).

Table 5 lists the values scaled by the factor 0.89, as proposed by Pople et al.[22] of the vibrational frequencies calculated at the HF/6-31G(d,p) level for reactants and transition states. The imaginary frequency involves the antisymmetric stretching C−H−Cl group and is related to the width of the barrier in the direction of the reaction coordinate. Compared to previous studies using a very sophisticated level of theory for H transfer reactions,[23,24] our values are much too high. Therefore, when the tunneling correction to the rate constants is calculated, these values will be scaled as explained later in the paper.

(ii) Reaction Enthalpies. The reaction enthalpies, ΔH_{298}, calculated using basis sets of increasing size are displayed in Table 6 and compared with the corresponding available experimental values obtained from heats of formation listed in ref 10. It can be observed that the increase of the basis set from a double to a triple ζ and the addition of polarization functions really improve the reaction enthalpies, ΔH_r. Finally,

TABLE 4: Optimized Geometries for Haloethanes of the Type CH_3CX_3 (Where X = F or/and Cl) and Transition States at the HF/6-31G(d) Level of Calculations (for the Transition States, the Lengths of Breaking C−H Bond and Forming H−Cl Bond Are Written in Italic Characters)

		X_3CCH_3	$X_3CC(H_2)-H-Cl$	*L*
CH_3CCl_3	*r*(*CH*$_1$)	1.081	*1.403*	*1.58*
	r(*H···Cl*)		*1.469*	
	r(CC)	1.521	1.507	
	r(CCl)	1.778	1.769	
	r(CH)	1.081	1.077	
	θ(HCC)	109.5	114.1	
	θ(H$_1$CC)	109.5	109.4	
	θ(ClCC)	109.9	110.6	
	dih(HCCCl)	180.0	180.0	
CH_3CCl_2F	*r*(*CH*$_1$)	1.080	*1.410*	*1.68*
	r(*H···Cl*)		*1.461*	
	r(CC)	1.511	1.506	
	r(CF)	1.336	1.340	
	r(CCl)	1.774	1.764	
	r(CH)	1.082	1.077	
	θ(H$_1$CC)	110.8	109.8	
	θ(HCC)	108.6	113.8	
	θ(FCC)	109.3	107.2	
	θ(ClCC)	111.4	111.6	
	dih(HCCF)	180.0	180.0	
	dih(HCCH$_1$)	120.5	112.5	
CH_3CClF_2	*r*(*CH*$_1$)	1.083	*1.411*	*1.68*
	r(*H···Cl*)		*1.460*	
	r(CC)	1.504	1.501	
	r(CF)	1.328	1.323	
	r(CCl)	1.775	1.761	
	r(CH)	1.081	1.077	
	θ(HCC)	110.0	115.4	
	θ(H$_1$CC)	107.9	107.9	
	θ(FCC)	110.6	110.4	
	θ(ClCC)	112.6	113.0	
	dih(HCCF)	180.0	180.0	
	dih(HCCH$_1$)	120.0	110.4	
CH_3CF_3	*r*(*CH*$_1$)	1.082	*1.411*	*1.68*
	r(*H···Cl*)		*1.460*	
	r(CC)	1.499	1.499	
	r(CF)	1.325	1.320	
	r(CH)	1.082	1.076	
	θ(HCC)	1.09.4	106.3	
	θ(H$_1$CC)	109.4	114.5	
	θ(FCC)	111.6	110.1	
	tor(HCCF)	180.0	180.0	

TABLE 5: Calculated HF/6-31G(d) Vibrational Frequencies (cm^{-1}) for Reactants and Transition States (Scaled by the Factor 0.89)

CH_3CCl_3	237, 237, 295, 333, 333, 338, 507, 731, 731, 1042, 1089, 1089, 1399, 1447, 1447, 2887, 2965, 2965
TS	*i1868*, 55, 71, 191, 237, 277, 330, 341, 437, 458, 522, 729, 742, 902, 981, 1056, 1098, 1147, 1409, 2948, 3039
CH_3CCl_2F	254, 261, 288, 361, 385, 419, 569, 755, 939, 1093, 1104, 1186, 1400, 1444, 1447, 2886, 2957, 2974
TS	*i1860*, 53, 70, 202, 258, 332, 376, 419, 449, 451, 586, 758, 899, 938, 991, 1098, 1145, 1199, 1409, 2953, 3047
CH_3CClF_2	243, 292, 325, 412, 420, 520, 658, 900, 980, 1120, 1227, 1231, 1409, 1445, 1445, 2886, 2958, 2973
TS	*i1856*, 46, 65, 212, 316, 316, 389, 402, 446, 458, 526, 674, 850, 927, 957, 996, 1213, 1242, 1254, 1413, 2961, 3078
CH_3CF_3	223, 348, 348, 520, 520, 575, 808, 974, 974, 1259, 1259, 1272, 1425, 1448, 1448, 2889, 2964, 2964
TS	*i1852*, 48, 71, 270, 335, 423, 436, 520, 533, 584, 815, 862, 932, 994, 1094, 1228, 1279, 1279, 1424, 2957, 3047

the best energy values, the PMP2/6-311G(2d,2p)//HF/6-31G-(d) energies, are corrected using equivalent isodesmic reaction processes explained in ref 6, namely, $CH_3 + CX_3CH_3 \rightarrow CH_4 + CX_3CH_2$. These values are presented in Table 6 as ΔH_r-(ISO). These last values will be used in the ISO-M method to determine the activation enthalpies. BAC-MP4 enthalpies, also listed in Table 6, give reasonable values with respect to experimental ones obtained from heats of formation taken from ref 10. In the case of the reaction involving CH_3CCl_2F, the heat of formation of CH_3CCl_2F itself and of the radical product CH_2CCl_2F are not known and have been calculated by the Melius BAC-MP4 method[21] to be -79.67 ± 1.11 and -27.02 ± 1.61 kcal mol^{-1}, respectively. If we now look for the trends along the series, it can be observed from Table 6 that the replacement of a chlorine atom by a fluorine one does not introduce a large change in the experimental values of the reaction enthalpies ΔH_r, at least for the first and second substitutions (less than 1 kcal mol^{-1}). These changes are much smaller than the changes recorded in the methane series, from $\Delta H_r = -8.4$ kcal mol^{-1} in the case of $CHCl_3$ to $\Delta H_r = +3.7$ kcal mol^{-1} for CHF_3. This situation is related to the fact that the inductive effect is much weaker for a change of a substituent on a β position with respect to a given center than on an α one.

(iii) Kinetic Parameters. The activation barriers E_a (Table 7) are calculated from the electronic energies corrected by the zero vibrational and thermal energies. From Table 7, it can be seen that the correlation energy due to the presence of polarization functions in the basis set lowers the activation barriers. The PMP2/6-311G(2d,2p)//HF/6-31G(d) energies (hereafter, we will refer to them simply as PMP2) are still too high. We had them corrected using the ISO-M method. Starting from PMP2 activation barriers, E_a(PMP2), and reactions enthalpies, ΔH_r(PMP2), we first look for the intrinsic energy E_{int} according to the Marcus relationship:

$$E_a = E_{int} + \frac{\Delta H_r}{2} + \frac{\Delta H_r^2}{16E_{int}} \qquad (6)$$

Since we have to deal with a C−H bond breaking with a similar atomic environment, the four E_{int} values are close together (respectively, from Cl_3 to F_3: 4.33, 3.73, 3.64, and 4.88 kcal mol^{-1}). Two ways are then possible: (i) one is to take each of these E_{int} values in the calculation of E_a, or (ii) the other way is to use the arithmetic average value $\langle E_{int} \rangle = 4.15$ kcal mol^{-1} of each of the reactions studied here. Then, E_{int} (or $\langle E_{int} \rangle$) and ΔH_r(ISO) are used within the same relationship (6) to give the corrected activation barriers E_a(ISO-M) that are listed in the fifth row of Table 7. In both cases, the resulting values are in good agreement with the experimental ones. Conversely, the E_a(BAC-MP4) values are higher than the E_a(ISO-M). But, with both approaches, the trends are the same. All of these E_a values are close together like the ΔH_r results, in agreement with the Hammond's postulate.[26] The rationale which governs the good agreement between theory and experiment has been presented in our previous paper[6] and will be briefly summarized here. As for the $CHX_3 + Cl$ series studied before, there exists a weak quadratic correlation between E_a and ΔH_r values calculated at various levels. This suggests that the Evans−Polanyi linear correlation between E_a and ΔH_r does not hold for either the substituted methanes or ethanes reacting with chlorine atom. Figure 8 shows an example for these quantities both calculated at the MP2/6-311G(2d,2p) level. This seems to justify the use of Marcus equation (6) in the ISO-M method.

The activation entropies $\Delta S^{\ddagger}(298)$ have been calculated using the HF/6-31G(d) geometries and the vibrational frequencies scaled by a factor 0.89 as recommended by Pople.[22] Using these $\Delta S^{\ddagger}(298)$ and conventional transition state theory, we have calculated the preexponential *A*-factors for each of the reactions in the series. Table 8 gathers the values of calculated molar entropies for reactants and transition states, the resulting

TABLE 6: Reaction Enthalpies ΔH_r(298K) (kcal mol^{-1}) for the Five Hydrogen Transfer Reactions Calculated at Various Levels of Theory Including the Sum of Thermal Energies at 298 K (Zero-Point + Thermal Energy Corrections)

	CH_3CCl_3	CH_3CCl_2F	CH_3CClF_2	CH_3CF_3
PMP2/6-31G(d,p)//HF/6-31G(d)	−4.62	−3.53	−3.96	−2.46
PMP2/6-311G(2d,p)//HF/6-31G(d)	2.69	3.02	3.47	4.58
PMP2/6-311G(2d,2p)//HF/6-31G(d)	2.52	4.01	4.49	5.63
BAC-MP4	1.30	1.60	2.30	3.59
ISO-M	1.60	1.92	2.41	3.55
experiment[a]	0.0	unknown	1.0	4.0

[a] Based on ΔH_f° at 298 K for CH_3CX_3, CH_2CX_3, and HCl from ref 10.

TABLE 7: Activation Energies E_a (kcal mol^{-1}) for the Five Hydrogen Transfer Reactions Calculated at Various Levels of Theory Including the Sum of Thermal Energies at 300 K (Zero-Point + Thermal Energy Corrections + Room Temperature)

	CH_3CCl_3	CH_3CCl_2F	CH_3CClF_2	CH_3CF_3
PMP2/6-31G(d,p)//HF/6-31G(d)	12.33	12.58	12.65	14.36
PMP2/6-311G(2d,p)//HF/631G(d)	7.56	7.86	8.04	9.89
PMP2/6-311G(2d,2p)//HF/6-31G(d)	5.68	6.00	6.23	8.10
BAC-MP4	8.25	8.57	8.54	10.43
ISO-M	5.17 (4.99)	4.75 (5.17)	4.94 (5.44)	6.82 (6.11)
experiment	3.6[a]	4.4[a]	4.8[a]	7.9[b]

[a] This work. [b] Reference 25. The values in parentheses are calculated using the average value of E_{int} as explained in the text.

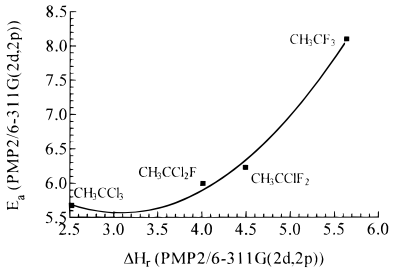

Figure 8. Quadratic correlation between the PMP2 values of the activation energies, E_a(PMP2/6-311G(2d,2p)) versus the reaction enthalpies ΔH_r(PMP2). Units for E_a and ΔH_r are kcal mol^{-1}.

TABLE 8: Entropies of Reactants (S), Transition States ($S^\ddagger$), Activation Entropies ($\Delta S^\ddagger$) (cal mol^{-1} K^{-1}), Preexponential Factors (A), and Rate Constants (cm^3 molecule^{-1} s^{-1}) Calculated at 298 K

	S	$S^\ddagger$	$\Delta S^\ddagger$	$A \times 10^{12}$	$A_{exp} \times 10^{12}$
Cl	39.5				
CH_3CCl_3	74.96	90.42	−24.04	7.5	2.8[a]
CH_3CCl_2F	74.78	88.36	−25.92	2.9	3.0[a]
CH_3CClF_2	72.30	86.50	−25.30	4.3	1.5[a]
CH_3CF_3	67.59	83.87	−23.22	12.3	17.3[b]

[a] This work. [b] Reference 24.

activation entropies and the preexponentional A-factors calculated at 298 K. Compared to the experimental values determined in this work over a limited temperature range, the A-factors are in good agreement, confirming the validity of the characteristics of the transition state formed by the calculations. The rate constants can then be easily calculated from these A and E_a values.

(iv) 1D Tunneling Correction. When dealing with a hydrogen transfer in a chemical reaction, it is a rather common practice to try to evaluate how the tunneling effect enhances the rate of reaction. Tunneling has been a well-known problem since the early days of quantum mechanics. However, this problem is far from being definitely solved in a full 3D physical space, and its importance in chemistry is still the subject of misunderstandings. A good review of this problem in bimolecular reactions was written some years ago by Schatz.[27] It is clear that a reliable determination of the transmission factor implies a full quantum 3D approach. This kind of approach is only possible at the present time for some three-atom reactions and for a four-atom process like $H_2 + OH$.[28] Approximate methods (some of them are based on reaction path determination) allow accurate evaluation of the tunneling factor (see for instance the work of Truhlar et al.[29−31]). Due to the rather large size of the systems studied here, we decided to estimate the tunneling factor (or transmission coefficient) using only an one-dimensional (1D) approach in order to compare the change of the tunneling effect in the series of interest. Such a calculation is based on a modeling of the reaction energy profile by an unsymmetrical Eckart potential characterized by the forward and backward barrier heights V_1 and V_2 in the entrance and exit channels, respectively (see figure included in Table 11 of ref 6).

TABLE 9: Imaginary Frequencies ν^* (cm^{-1}), V_1 (kcal mol^{-1}), V_2 (kcal mol^{-1}) and Γ^*

reactants	ν^*	V_1	V_2	Γ^*
CH_3CCl_3	1393	3.39	4.99	5.31
CH_3CCl_2F	1387	3.25	5.17	5.13
CH_3CClF_2	1384	3.03	5.44	4.94
CH_3CF_3	1381	2.56	6.11	4.32

We used the development of Johnston et al.[32−35] for the evaluation of the ratio Γ^* between the quantal and classical expressions of the thermal rate constant, i.e.,

$$\Gamma^* = \frac{k_{quantal}}{k_{classical}} = \frac{\exp[V_1/k_BT]}{k_BT}\int_{\epsilon_0}^{\infty}\kappa(E)\exp\left[-\frac{E}{k_BT}\right]dE \quad (7)$$

with $\kappa(E)$, the transmission coefficient defined according to formula 13 of ref 36. In formula 7, $\epsilon_0 = 0$ if $V_2 \geq V_1$ and $\epsilon_0 = V_1 - V_2$ if $V_2 < V_1$. This last situation is encountered here, since all the reactions are endothermic. Table 9 contains the modulus ν^* of the imaginary frequency at the saddle point, the barrier heights V_1 and V_2, and the value Γ^* of the integral 7 for each reaction studied. The frequencies are scaled by the same factor as that in ref 6 (which corresponds to ν^*(UHF)/ν^*(PMP2) = 0.7456 for the $ClF_2C-H-Cl$ transition state). We observe that all of the Γ^* values are around 5. Therefore, this correction may represent a significant part of the rate constant at 300 K. However, this kind of result should be taken with caution due to the assumptions used in the calculations and the uncertainties of experimental values. Finally, taking into account the tunneling effect, the corrected values of the rate constants at 300 K are displayed in Table 10. Comparisons can be done with experimental values and calculated rate constants with tunneling correction. Rate constants at other temperatures can be calculated in the same way, if desired.

TABLE 10: Rate Constants Calculated at 298 K (cm^3 $molecule^{-1}$ s^{-1}) Using the ISO-M Values of Activation Energies and Preexponential Factors

reactants	k_{calc}	$\Gamma^* k_{calc}$	k_{exp}
CH_3CCl_3	1.3×10^{-15}	6.8×10^{-15}	7.1×10^{-15}
CH_3CCl_2F	1.0×10^{-15}	5.0×10^{-15}	1.8×10^{-15}
CH_3CClF_2	1.1×10^{-15}	5.3×10^{-15}	4.7×10^{-15}
CH_3CF_3	1.3×10^{-16}	5.7×10^{-16}	2.7×10^{-17}

Conclusion

Arrhenius expressions for metathesis reactions of Cl atoms with CH_3CCl_3, CH_3CCl_2F (HCFC-141b), and CH_3CClF_2 (HCFC-142b) have been determined using the conventional DF/MS technique. Optimized pseudo-first-order conditions resulted in operation under excess Cl atom, as opposed to conventional excess reactant molecule. Wall loss and recombination of atomic chlorine (Cl + Cl + M) rate coefficients, k_w and k_r, respectively, were utilized in the calculation of the rate coefficients. Inclusion of Cl atom losses is shown to be important for the slower reactions, requiring longer reaction times. Arrhenius expressions are in good agreement with literature data, where available.

The characterization of the transition states for the abstraction of a hydrogen atom from each of CH_3CCl_3, CH_3CCl_2F, CH_3CClF_2, and CH_3CF_3 halogen-substituted ethanes (F,Cl) by chlorine atom attack has been done. The kinetic parameters (activation energies and preexponential factors) have been calculated by an ab initio method. The geometries have been optimized at the HF/6-31G(d) level of theory. Then the energies were calculated as single points at the PMP2 level with increasing basis sets. It is shown that a rather large basis set is necessary (6-311G(2d,2p)) to obtain really improved results for reaction enthalpies and activation energies. To obtain a better fit with experiment, energetic corrections have been added by means of the ISO-M method which corrects the reaction energies and uses the concept of intrinsic energy to deduce the activation barriers. The comparison with experimental activation energies shows a satisfying agreement, taking into account the uncertainties in both domains, and we can conclude that this last method gives semiquantitative results.

We have shown that a weak quadratic correlation (of Marcus type) between the activation barriers and the reaction enthalpies calculated by various methods is more suitable for analyzing the reactivity trends in the series of reactions between haloethanes and chlorine atoms than the linear correlation of Evans−Polanyi type.

The evolution of the energetics in the series of chlorofluoroethanes has been satisfactorily interpreted in terms of chlorine and fluorine substitutions. We have shown that the transition state geometric and electronic structures are related to the height of the barrier and to reaction enthalpies. The preexponential factors calculated for the four H-abstraction reactions by Cl atoms from the methyl group in the series $CH_3CCl_{3-x}F_x$ are in the same order of magnitude as the corresponding values measured in this work and by other authors in the case of CH_3CF_3.

Using these results, the rate constants calculated at room temperature and corrected for the tunneling effect are in acceptable agreement with experimental values measured in the same conditions, showing the predictive usefullness of quantum chemistry. It is worth noticing that the tunneling correction does not seem to be negligible at 300 K.

Acknowledgment. We are grateful to Dr. J. Franklin (Solvay) for providing samples of HCFC-141 and HCFC-142 without charge. We thank Prof. J. Peeters (University of Leuven) and Prof. H. Hippler (University of Karlsruhe) for their fruitful discussions. The calculations have been performed at the I.D.R.I.S. Computer Center (Orsay, France).

References and Notes

(1) Wallington T. J.; Hurley, M. D. *Chem. Phys. Lett*. **1992**, *189*, 437.

(2) Tuazon, E. C.; Atkinson, R.; Corchnoy, S. B. *Int. J. Chem. Kinet.* **1992**, *24*, 639.

(3) Sawerysyn, J.-P.; Talhaoui, A.; Mériaux, B.; Devolder, P. *Chem. Phys. Lett*. **1992**, *198*, 197.

(4) Warren, R. F.; Ravishankara, A. R. *Int. J. Chem. Kinet*. **1993**, *25*, 833.

(5) Talhaoui, A.; Louis, F.; Mériaux, B.; Devolder, P.; Sawerysyn, J.-P. *J. Phys. Chem*. **1996**, *100*, 2107.

(6) Rayez, M.-T.; Rayez, J.-C.; Sawerysyn, J.-P. *J. Phys. Chem*. **1994**, *98*, 11342.

(7) Sawerysyn, J.-P.; Lafage, C.; Mériaux, B.; Tighezza, A. *J. Chim. Phys.* **1987**, *84*, 1187.

(8) Park, J. Y.; Slagle, I. R.; Gutman, D. *J. Chem. Phys*. **1983**, *87*, 1812.

(9) Talhaoui, A. Thèse, University of Lille I, 1995.

(10) DeMore, W. B.; Sander, S. P.; Golden, D. M.; Hampson, R. F.; Kurylo, J.; Howard, C. J.; Ravishankara, A. R.; Kolb, C. E.; Molina, M. J. *Chemical Kinetics and Photochemical Data for Use in Stratospheric Modeling*; Evaluation No. 11, Publication 94−26, Jet Propulsion Laboratory: Pasadena, CA 1994.

(11) Atkinson, R.; Baulch, A. R.; Cox, R. A.; Hampson, R. F.; Kerr, J. A.; Troe, J. *J. Phys. Chem. Ref. Data* **1992**, *21* (6), 1125.

(12) Wine, P. H.; Semmes, D. H.; Ravishankara, A. R. *Chem. Phys. Lett*. **1982**, *90*, 128.

(13) Cillien, C.; Goldfinger, P.; Huybrechts, G.; Martens, G. *Trans. Faraday Soc*. **1967**, *63*, 1631.

(14) Tschuikow-Roux, E.; Neizielski, J.; Faraji, F. *Can. J. Chem*. **1985**, *63*, 1093.

(15) Jourdain, G. L.; Poulet, G.; Barassin, J.; Lebras, G.; Combourieu, J. *J. Pollut. Atmos*. **1977**, *75*, 256.

(16) Dong, Z. P.; Schneider, M.; Wolfrum, J. *Int. J. Chem. Kinet*. **1989**, *21*, 387.

(17) Frisch, M. J.; Trucks, G. W.;. Head-Gordon, M.; Gill, P. M. W.; Wong, M. W.; Foresman, J. B.; Johnson, B. G.; Schlegel, H. B.; Robb, M. A.; Replogle, E. S.; Gomperts, R.; Andres, J. L.; Raghavachari, K.; Binkley, J. S.; Gonzalez, C.; Martin, R. L.; Fox, D. J.; Defrees, D. J.; Baker, J.; Stewart J. J. P.; Pople, J. A. *Gaussian 92*, Revision E.2; Gaussian, Inc.: Pittsburgh, PA, 1992.

(18) Hariharan, P. C.; Pople, J. A. *Theor. Chim. Acta* **1973**, *28*, 213.

(19) Melissa, V. S.; Truhlar, D. G. *J. Chem. Phys.* **1993**, *99*, 1013.

(20) Marcus, R. A. *J. Phys. Chem*. **1968**, *72*, 891.

(21) (a) Book chapter by: Melius, C. F. *Thermochemical Modelling I. Application to Ignition and Combustion of Energetic Materials*; Chemistry and Physics of Energetic Materials; Kluwer Academic: New York, 1992; pp 21 . (b) Ho, P.; Melius, C. F. *J. Phys. Chem*. **1990**, *94*, 5120.

(22) Hehre, J. H.; Radom, L.; Shleyer, P. v. R.; Pople, J. A. *Ab initio Molecular Theory*; John Wiley and Sons, Inc.: New York, 1986.

(23) Truong, T. N.; Truhlar, D. G.; Baldridge, K. K.; Gordon, M. S.; Steckler, R. *J. Phys. Chem*. **1989**, *90*, 7137.

(24) Gonzalez-Lafont, A.; Truong, T. N.; Truhlar, D. G. *J. Chem. Phys*. **1991**, *95*, 8875.

(25) Tschuikow-Roux, E.; Yano T.; Neizielski, J. *Chem. Phys*. **1985**, *82*, 65.

(26) Hammond, G. S. *J. Am. Chem. Soc*. **1955**, *77*, 334.

(27) Schatz, G. C. *Chem. Rev*. **1987**, *87*, 81.

(28) (a) Zhang, D. H.; Zhang, J. Z. H. *J. Chem. Phys*. **1994**, *101* (2), 1146. (b) Zhang, D. H.; Zhang, J. Z. H.; Zhang, Y.; Wang, D.; Zhang, Q. *J. Chem. Phys*. **1995**, *102* (19), 7400.

(29) Skodje, R. T.; Truhlar, D. G.; Garrett, B. C. *J. Phys. Chem*. **1981**, *85*, 3019.

(30) Garrett, B. C.; Truhlar, D. G.; Wagner, A. F.; Dunning, T. H. *J. Phys. Chem*. **1983**, *78*, 4400.

(31) Garrett, B. C.; Truhlar, D. G. *J. Phys. Chem*. **1983**, *79*, 4931.

(32) Johnston, H. S.; Rapp, D. *J. Am. Chem. Soc*. **1961**, *83*, 1.

(33) Johnston, H. S.; Heicklen, J. *J. Phys. Chem*. **1962**, *66*, 532. Note that formula 15 of this paper should read as follows: $2\pi b = 2[\alpha_1(\zeta - 1) + \alpha_2]^{1/2}[\alpha_1^{-1/2} + \alpha_2^{-1/2}]^{-1}$.

(34) Johnston, H. S. *Gas phase reaction rate theory*; The Ronald Press Co.: New York, 1966.

(35) Brown, R. L. *J. Res. Natl. Bur. Stand* **1981**, *86*, 357.

(36) Cohen, N.; Benson, S. W. *J. Phys.Chem*. **1987**, *91*, 162.

JP9603243